Resources, Conservation & Recycling Advances 23 (2024) 200227

Contents lists available at ScienceDirect

Resources, Conservation & Recycling Advances

journal homepage: www.sciencedirect.com/journal/Resources-Conservation-and-Recycling-Advances

Recycling devulcanized EPDM to improve engineering properties of SBR rubber compounds

X. Colom [a,*], M. Marín [b], M.R. Saeb [c], K. Formela [d], J. Cañavate [a]

[a] Department of Chemical Engineering, ESEIAAT-UPC, Colom, 1, 08222, Terrassa, Spain
[b] Department of Mechanical Engineering, ETSEQ-URV, Països Catalans, 26, 45002, Tarragona, Spain
[c] Department of Pharmaceutical Chemistry, Medical University of Gdańsk, J. Hallera 107, 80-416, Gdańsk, Poland
[d] Department of Polymer Technology, Faculty of Chemistry, Gdansk University of Technology, Gabriela Narutowicza 11/12, 80–233, Gdansk, Poland

ARTICLE INFO

Keywords:
Devulcanized EPDM
Recycling
Materials characterization
Thermomechanical devulcanization
Microwave devulcanization

ABSTRACT

Ethylene propylene diene rubbers (EPDM) have gained substantial attention in automotive and industrial applications owing to their exceptional resistance against weathering and heat. Despite their advantages, the elastomeric nature of EPDM poses challenges in its recycling due to the presence of crosslinks in their chemical structure, preventing them from melting. To overcome this issue, devulcanized EPDM (EPDMd) has been developed, characterized by the effective breaking of these crosslinks. Our study focuses on common composites that include Styrene Butadiene Rubber (SBR), EPDM and silica, but with the incorporation of devulcanized EPDM (EPDMd).

We have studied the mechanical, thermal, structural and dielectric properties of SBR composites containing EPDMd at variable compositions (0, 20, 40, 50, 60 phr). Employing techniques such as Thermogravimetric Analysis (TGA), Fourier Transform Infrared Spectropy (FTIR), and Scanning Electronic Microscopy (SEM), we have explored the microstructural changes driving the macroscopic effects on the measured properties.

The results show that incorporating EPDMd improves the crosslinking degree and, at optimal 40 phr loading, significantly increases the mechanical properties of SBR matrix. The addition of SiO_2, in general, reduce tensile strength and elongation, while increasing the Young's modulus, except for compositions around 40 phr EPDMd. The dielectric measurements are in concordance with the previous data, showing a moderation of the Maxwell–Wagner–Sillars (MWS) effect due to SiO2 in highly filled EPDMd composites at 40 phr EPDMd.

1. Introduction

Utilizing waste and recycled rubbers (Wiśniewska et al., 2023) alongside fillers (Hejna et al., 2023) in rubber industry has become a route to preserve sustainability Ethylene propylene diene rubbers (EPDM) are best known polymers in automotive and industrial sectors due to their exceptional resistance against weathering and heat. Since their introduction to the market in the 1960s, EPDM elastomers have witnessed consistent growth, currently ranking third among synthetic elastomers. They dominate technical applications, excluding tires, with an impressive installed capacity of approximately 1.3 million tons (Welker et al., 2012). As of 2021, the Asia-Pacific region commanded the largest share of the EPDM market at 41.2 %, and this figure is anticipated to rise to 43.3 % by 2031. Notably, the North American market is poised for a 5.3 % growth, primarily propelled by the robust demand for EPDM in automotive and diverse industrial applications. The expanding automotive industry in the burgeoning economies of the BRIC countries is expected to significantly boost the global demand for EPDM in the coming years, further solidifying its position as a key player in the polymer industry (www.researchandmarkets.com, 2023). Utilization of EPDM extends far beyond the automotive sector. Particularly in Spain, Italy, the UK, and various Western European countries, there is a notable surge in its use for roofing and building waterproofing applications. These uses involve the incorporation of EPDM sheaths, resulting in a substantial consumption of this material (www.transparencymarketresearch.com, 2023).

The expansion of EPDM's applications has been propelled by the growing demand for superior elastomers possessing unique properties. This demand, in turn, has stimulated innovations in catalysts and manufacturing processes (Ravishankar, 2012). Given EPDM's

* Corresponding author.
E-mail address: xavier.colom@upc.edu (X. Colom).

https://doi.org/10.1016/j.rcradv.2024.200227

Available online 22 August 2024

significance and extensive production in today's market, there is a pressing need for the development of recycling processes tailored to handle EPDM waste. Recycling stands as the most environmentally responsible approach for the continued utilization of rubber in all its forms, EPDM being no exception. By optimizing the use of existing resources, the rubber industry can make significant strides toward a more sustainable environmental recovery, reinforcing its commitment to eco-friendly practices. EPDM, characterized by its inert nature and limited environmental impact, poses a unique challenge in the recycling due to its elastomeric properties. The presence of crosslinks within its chemical structure prevents it from melting, requiring innovative solutions. Various techniques have been proposed to overcome this issue, referred to as devulcanization. This process focuses on breaking the crosslinking while preserving the main macromolecular chains. Through devulcanization, the inherently crosslinked structure of EPDM is transformed into a morphology that is similar to that of a thermoplastic material, rendering it susceptible to recycling and subsequent revulcanization processes. This transformative step not only facilitates recycling but also allows for the ulterior restitution of the original crosslinked structure.

Several devulcanization methods have been explored, with ultrasonic devulcanization (Yun et al., 2003), thermomechanical devulcanization (Colom et al., 2021; Gschwind et al., 2023; Zoltán et al., 2021), and microwave devulcanization (de Sousa et al., 2022; Dubey et al., 2006) being as some of the most widely utilized techniques. The devulcanization process can be followed by blending with fresh material and subsequent re-vulcanization. This results in the formation of a new compound that can be tailored to specific requirements, all while exhibiting comparable or even enhanced properties. This innovative approach not only addresses the challenge of EPDM recycling, but also opens doors to the manufacturing of customized, sustainable materials with diverse applications. EPDM exhibits compatibility with a wide array of elastomers and thermoplastics, including styrene butadiene rubber (SBR). Blending EPDM with SBR offers an economically viable solution while retaining several key mechanical properties of EPDM (Zanchet et al., 2012). This synergy has made the SBR/EPDM combination a staple in various engineering applications, such as tires, conveyor belts, seals, electrical insulators, gaskets, and more, underscoring its widespread use (Graf, 2024). Such an extensive application motivated the selection of SBR/EPDM blend for the present study. In these elastomeric composites, silica is frequently incorporated due to its ability to enhance wear resistance, stiffness, durability, and tear resistance of the final product. Moreover, silica plays a pivotal role in promoting the dispersion and stability of the compound, thereby elevating material quality and consistency (Lee et al., 2020). The properties of these elastomeric composites are profoundly affected by the quantity and size of silica particles. Smaller silica particles contribute to enhanced dispersion within the compound, leading to superior mechanical strength. Additionally, utilizing silica with a high specific surface area further augments the compound's properties, showcasing the impact that particle size and surface area can have on the final product.

The proposed SBR/EPDMd blends are produced using conventional equipment and techniques. The rubber is cured with standard vulcanization systems and conditions. Utilizing devulcanized EPDMd is expected to enhance the crosslinking and interaction between the two polymers in the blend.

In this study, our objective was to collect first set of data on the mechanical, thermal, and dielectric characteristics of composites comprising SBR and a type of EPDM, which underwent a devulcanization process within the laboratory, at varying contents. Recognizing the significant impact that silica, a commonly used additive in such materials, could have on these properties, we have also considered its potential effects. To investigate deeper into these composites, we employed analytical techniques such as TGA, FTIR, and SEM. By doing so, we aimed to research the microstructural changes underlying the observable macroscopic effects in the measured properties. This approach was undertaken with the objective of enhancing our comprehension of the nature and behavior of these materials, in order to use as a component in automotive industry. Through this analysis, we sought to shed light on the interactions and transformations occurring at a microscopic level, providing valuable insights that contribute to a deeper understanding of these composite materials.

2. Materials and methods

2.1. Materials

SBR stabilized with Butylated Hydroxytoluene (BHT) antioxidant 0.375 %, bound styrene 24 %, organic acid 5.5 % and Mooney Viscosity 52 (ML+1@100 °C) was supplied by VIGAR Rubí Barcelona (Spain).

Micro/nanoparticles of SiO2 (83 % particle size lower to 150 μm and 180 m^2/g of specific area) and waste EPDM of commercial, industrial and residential roofing origin were supplied by Firestone Building Products Terrassa Barcelona (Spain).

The additives and agents used for curing, the vulcanization accelerators (TBBS- N-tert-butyl-2-benzothiazole sulfonamide, TMTD - tetramethylthiuram disulfide), the carbon black N550 (ASTM D1765), stearic acid, zinc oxide and sulfur with technical purity, were supplied by VIGAR Rubí Barcelona (Spain).

2.2. Devulcanization of EPDM

Devulcanization process of EPDM by combined thermomechanical/microwave procedures, has been developed according to the procedure already tested and published by our group in a previous paper (Colom et al., 2021).

The thermo-mechanical treatment is carried out in a Brabender plastograph at 80 °C and 80 rpm, including the addition of 2phr of benzoyl peroxide (devulcanizing agent) which helps the thermomechanical devulcanization. The microwave irradiation takes place in a prototype microwave oven with a motorized stirring adapted in our laboratory. The microwaves devulcanization process was performed setting the magnetron power to 700 W, 80 rpm of the stirrer and 3 min of MW exposure.

The resulting material after this process has been named EPDMd.

2.3. Samples preparation

The formulations of the elastomeric composites are shown in Table 1.

The mixing process consists of three steps. In the initial step, there is a preliminary plasticization of the fresh SBR elastomer which lasts for 2 min. This is followed by a mixing stage with EPDMd, 30phr of carbon black and 30phr of SiO_2 are blended for 4 min. Finally, the sulfur curing system (zinc oxide 5.0 phr; stearic acid 3.0 phr; TBBS 1.0 phr; TMTD 0.25 phr; sulfur 2.0 phr) is added to the blend and mixed for 2 min allowing the revulcanization process to take place.

The rubber ingredients were mixed in a Plasticorder internal mixer (Brabender GmbH & Co. KG, Duisburg, Germany) at 80 °C and 80 rpm. The order of appearance of the components presented in Table 1 (left to right) also reflects the order of mixing. The devulcanized EPDM content in the samples was 0, 20, 40,50 and 60 parts per hundred of rubber (phr).

Two batches of the mix cited above are necessary to create a suitable sample plate of the polymer. These two batches are recombined in a two-roll mill Collin Teach-line. The resulting material is subsequently molded in a Collin P 200 E hot plate press at 160 °C and 200 bar. These conditions correspond to the optimum cure time (t90) determined by the vulcanization characteristics of vulcanizable rubber composites according to ASTM D2084, with an Oscillating Disc Rheometer R 100, Monsanto, (Akron, Ohio, USA), at 162 ± 1 °C. After this time, the mold is removed carefully from the press with Kevlar gloves and quickly taken to cool. Finally, the mold is separated from the part, which is now ready

Table 1
SBR-based rubber composites containing devulcanized EPDM and their abbreviations (values in phr).

Abbreviation	SBR	EPDMd	SiO_2	CB	ZnO	StA	TBBS	TMTD	S
SBR Ref	100	0	0	30	5	3	1	0,25	2
SBR EPDMd20	100	20	0	30	5	3	1	0,25	2
SBR EPDMd40	100	40	0	30	5	3	1	0,25	2
SBR EPDMd50	100	50	0	30	5	3	1	0,25	2
SBR EPDMd60	100	60	0	30	5	3	1	0,25	2
SBR SiO_2Ref	100	0	30	30	5	3	1	0,25	2
SBR EPDMd20 SiO_2	100	20	30	30	5	3	1	0,25	2
SBR EPDMd40 SiO_2	100	40	30	30	5	3	1	0,25	2
SBR EPDMd50 SiO_2	100	50	30	30	5	3	1	0,25	2
SBR EPDMd60 SiO_2	100	60	30	30	5	3	1	0,25	2

to shape the test samples with a J.BOT Instruments S.A. (Barcelona, Spain) test cutter, designed to obtain dumbbell-shaped test samples according to the specifications of the ASTM-D- 412-98.

2.4. Measurements

The tensile properties of the vulcanized rubber SBR EPDMd composites, were evaluated following the ISO 37 standard. Testing was conducted using a high-precision Instron 3366 testing machine from the USA, boasting a cell load capacity of 20 kN. The tensile tests were executed at a constant cross-head speed of 500 mm/min, maintaining a controlled environment with a relative humidity (RH) of 50±5 % and a temperature of 23±2 °C.

For hardness assessments, a Zwick 3130 durometer Shore A from Germany was used, following the ISO 7619-1 standard. To ensure precision and reliability, both tensile and hardness evaluations were based on an average of five measurements per sample. This methodology guarantees the accuracy and consistency of the obtained results, providing a robust foundation for the analysis of the material's mechanical properties.

Swelling degree of elastomers compounds (0.2 g samples) was determined by equilibrium swelling in toluene (room temperature) after immersing the samples in the medium for 72 h. Swelling degree was calculated in accordance with the formula (1):

$$Q = \frac{m_t - m_o}{m_o} \times 100\% \quad (1)$$

where: Q – swelling degree; m_t – mass of the sample swollen (g); m_o – initial mass of sample (g).

The crosslink density was determined according to ASTM D6814-02 standard method through swelling measurements of the rubber composites which were let to swell in cold toluene for 72 h refreshing the solvent every 24 h (Zoltán et al., 2021). The Flory Rehner equation (Flory and Rehner 1943) was used to calculate the crosslink density.

The χ interaction parameter between rubber and swelling solvent was set equal to 0.377 (Marzocca, 2007) and toluene as solvent. Kraus correction model was applied due to the presence of carbon black as a filler (Kraus, 1963). The carbon black density was chosen equal to 1.85 g/cm^3 and the K constant was chosen to be 1.17 (Hrnjak-Murgić, 1997). The Eqs. (2) and (3) were used for cross-link density calculations.

$$\nu_e = \frac{-\left[\ln(1 - V_r) + V_r + \chi V_r^2\right]}{\left[V_1\left(V_r^{1/3} - V_r/2\right)\right]} \quad (2)$$

Where: ν_e – cross-link density, mol/cm^3; V_1 – solvent molar volume (toluene = 106.2, cm^3/mol) and V_r means the volume fraction of rubber in the swollen sample, which can be determined with Ellis and Welding equation (Ellis and Welding, 1964).

$$V_r = \frac{\frac{m_p}{\rho_p}}{\frac{m_p}{\rho_p} + \frac{m_s}{\rho_s}} \quad (3)$$

where: m_p – the weight of the dry polymer; ρ_p – the density of the dry polymer g/cm^3; m_p – the weight of solvent absorbed by polymer; ρ_s – the density of the solvent.

Cross-link density with Kraus correction was calculated according Eqs. (4) and (5):

$$\nu_{\text{after correction}} = \frac{\nu_e}{1 + K \times \Phi} \quad (4)$$

$$\Phi = \frac{\varphi_f \times \rho_r \times m_0}{\rho_f \times m_{dry}} \quad (5)$$

Where, ν_e – the measured chemical cross-link density, mol/cm^3; $\nu_{\text{after correction}}$ – the actual chemical cross-link density, mol/cm^3; K – constant characteristic of the filler but independent of the solvent; ϕ_f – the volume fraction of filler in the sample which is calculated; ρ_r – the density of studied compound, g/cm^3; m_0 – the weight of sample before extraction; ρ_r – the density of filler, g/cm^3; m_{dry} – the weight of sample after extraction.

The density of the samples was measured based on the Archimedes method, as described in ISO 2781. Accordingly, all measurements were carried out at room temperature in methanol medium.

TGA was performed on a Perkin Elmer TGA 8000 apparatus (USA). SBR/GTR composite weighing approximately 10 mg was placed in a corundum dish. The measurement was conducted in the temperature range 30–800 °C and under oxidant atmosphere (30 ml/min), at a heating rate of 20 °C/min. Obtained results are the average of three measurements per sample. Likewise, a nitrogen flow of 20 ml/min has also been used to prevent the gasses generated during the thermooxidative decomposition process from depositing in the thermo-balance and potentially damaging it.

The morphology of SBR EPDMd fracture surfaces created by the tensile test of the composites at the speed of 500 mm/min was observed with a JEOL 5610 scanning electron microscope (Japan). Before observation the samples were covered with a fine gold–palladium layer in order to increase their conductivity in a vacuum chamber.

Chemical structure of SBR EPDMd composites was determined using FTIR-ATR analysis performed by means of a Spectrum Two spectrometer from Perkin Elmer (USA). The device had an ATR attachment with a diamond crystal. Spectra were registered at 2 cm^{-1} resolution and 40 scans in the range of 500–3500 cm^{-1}, in which the compound signals related to different deformation bands can be observed.

For the dielectric characterization, an impedance spectroscopy machine for Dynamic Electrical Analysis (DEA) and a Novocontrol test rig were used. A sample 2.5 cm in diameter and 0.1 mm thick was used, which was placed on the measuring electrodes of the instrument.

3. Results and discussion

3.1. Physical and mechanical properties

Fig. 1, compares the tensile strength of samples with different contents of EPDMd with silica and without silica. The inclusion of SiO_2 in the SBR EPDMd samples results in a reduction in tensile strength (TS) values. This decrease is attributed to SiO_2 micro-particles, which disrupt

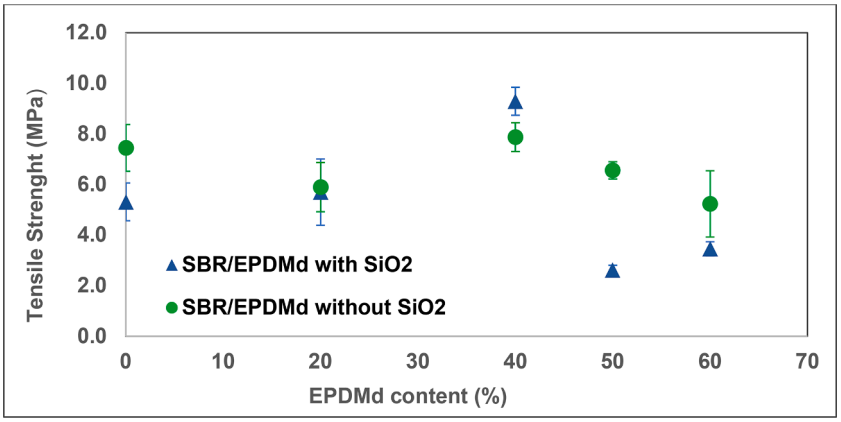

Fig. 1. Tensile strength of samples with different contents of EPDMd.

the continuity of the SBR matrix and create stress points within the material. However, the SEM results presented subsequently, indicate that SiO_2 has much more affinity for the devulcanized EPDM particles than for the SBR matrix. We believe that the BPO used in the devulcanization process, reacts with devulcanized EPDM (Rooj et al., 2011), inducing affinity to SiO_2. The affinity leads to an attraction of the SiO_2 particles for the EPDMd phase which causes an effect on the properties.

The addition of EPDMd enhances the tensile strength (TS) up to a content level of 40 phr. However, when the EPDMd content exceeds this threshold, the TS begins to decrease. The decrease is much more significant in the samples containing SiO_2 than in the samples without it. This higher decrease found in the case of samples above 40phr is attributed to the surrounding of the EPDMd by the SiO_2 generating a continuous phase conducting to the formation of big stress areas that cause a faster break of the samples.

A interesting phenomenon is observed in the SBR/ EPDMd40 samples: the sample incorporating SiO_2 exhibits a higher tensile strength (TS) value than its SiO_2-free counterpart. This can be attributed to the relatively low dispersion degree of EPDMd, which is enveloped by SiO_2. This phenomenon aligns with findings in previous publications where it was demonstrated that the EPDMd tends to form agglomerates (Lee et al., 2020). These SiO_2-wrapped agglomerates, while not quantitatively sufficient to establish a continuous phase, resist breakdown more effectively, especially when compared to higher EPDMd content samples.

However, due to the presence of these agglomerates, the dispersed SiO_2 content in the matrix is reduced. Consequently, this results in a lower number of stress zones.This reduction in stress zones contributes to a higher tensile strength value than that observed in the sample lacking SiO_2 (refer to Fig. 3).

Fig. 2 presents a comparison of SBR EPDMd samples, this time considering Young's modulus at 100 % elongation, with and without SiO_2, in relation to the EPDMd content (phr).

Samples with SiO_2 (blue triangle) have a higher Young's modulus than the samples without SiO_2 (green circles). Likewise, to the TS case, there is an increase of the studied property until the amount of EPDMd reaches the 40phr and then there is a significant reduction in the samples without SiO_2. The decrease in the samples with SiO_2 is much more attenuated, which means that the stiffness is still preserved even at high EPDMd contents. The addition of SiO_2 improves the stiffness of the sample and this causes this increase in Young's modulus. This is an usual effect of silica addition. When the EPDMd particle content exceeds 40 phr (SBR EPDMd60), the EPDMd agglomerates dispersed in the SBR matrix generate a continuous phase which causes a loss of stiffness and a slight reduction of the Young's modulus (see Fig. 3)

Fig. 4, which displays the evolution of the elongation at break (EaB) as a function of the content of EPDMd, shows that the samples containing SiO_2 (blue triangles) exhibit a lower elongation at break than the samples without SiO_2. These results are in accordance with the patterns observed in the tensile strength (TS) results and could be anticipated.

The samples including SiO_2 introduce more stress areas in the SBR/ SiO_2 interface. As previously mentioned, the EPDMd particles (devulcanized using BPO) have more affinity for SiO_2 than for the SBR matrix. However, as in the TS results, the SBR EPDMd40 SiO_2 sample has a higher elongation at break than the sample without SiO_2. The same reasoning used before is applicable here, the relatively high content of EPDMd is recovered in SiO_2, the interaction is enhanced and therefore the EaB improves. As reported in previous publications (Colom et al.,

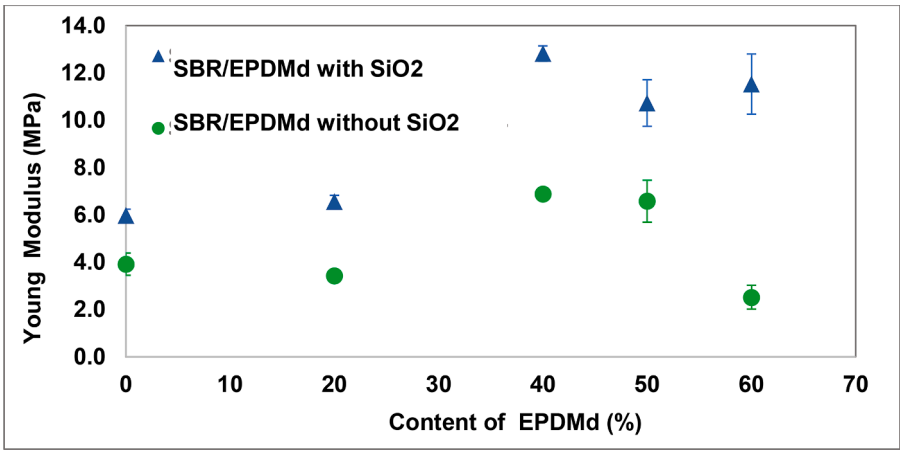

Fig. 2. Young modulus of samples with different contents of EPDMd.

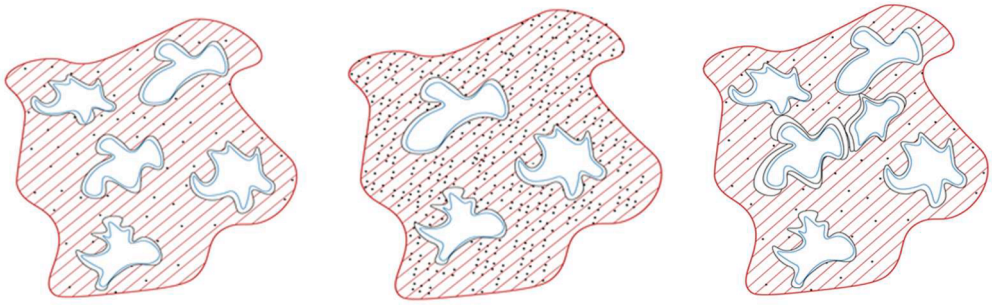

Fig. 3. Scheme of SBR EPDM20 SiO2; SBR EPDM40 SiO2 and SBR EPDM60 SiO_2 (continuous phase).

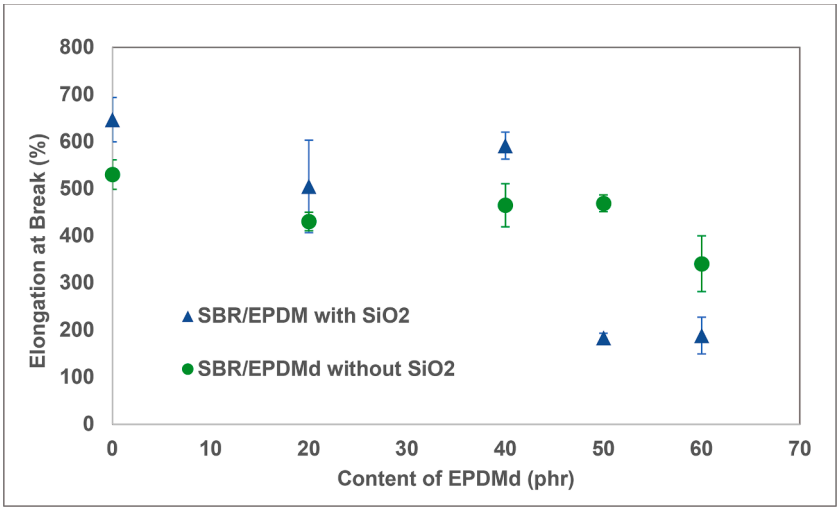

Fig. 4. Elongation at break of samples with different contents of EPDMd.

2023), when the EPDMd content is higher, it can generate a continuous phase, then, fracture areas appear and the EaB drops drastically.

Table 2 presents the numerical values of the mechanical properties as well and includes results for hardness, crosslinking (CLK) and swelling degree (SD). There exists a correlation between crosslinking (CLK) and swelling degree (SD), with higher crosslinking corresponds lower swelling degree. Increasing the cross-link density implies a tighter polymeric network, that does not allow the solvent entering within the structure and therefore, less swelling will result.

In the samples without SiO_2 it is observed that the CLK increases with EPDMd content. EPDMd has a higher propensity for crosslinking compared to SBR, because of its more accessible unsaturated sites. The samples including SiO_2 present the same tendency. CLK increases and SD decreases as a function of EPDMd content, but compared to the samples without SiO_2, the values of CLK are lower and SD higher.

Previous studies have emphasized the critical effect on the crosslinking caused by the presence of SiO_2. According to Zedler et al. (Zedler et al., 2021) the vulcanization mechanism is mainly affected by two factors involving SiO_2: i) the physical inhibition caused by SiO_2, which reduces the mobility of the SBR and EPDMd chains and prevents part of the elastomers from participating in the vulcanization and ii) the effect of SiO_2 groups, which favours the formation of radicals because of its -OH surface groups. According to Kazemi et al. these hydroxyl groups also favor the agglomeration of SiO_2 (Kazemi et al., 2019). In their study on natural rubber hybrid composites filled with maple/silica/carbon black (Kazemi et al., 2019), noted that the inclusion of 30phr of SiO_2 was related to the formation of hydrogen bonding between the silanol groups present on the silica surface. This phenomenon was considered responsible for the observed increase of Swelling Degree when adding silica (321 % with SiO_2 compared to 169 % without SiO_2).

An increase in hardness is observed as a function of the EPDMd content and the SiO_2 content, as appear in table 2. A synergistic effect is

Table 2
Mechanical properties of the samples.

Abreviattion samples	Tensile strenght (MPa)	Elongation at break (%)	Young modulus (MPa)	Hardness (shore A)	Crosslinking (mol/cm^3)	Swelling degree (%)
SBR Ref	7,45 ± 0,926	644,21 ± 47,0	3,91 ± 0,472	48,5 ± 0,83	$6{,}04{\cdot}10^{-4}$	169
SBR SiO_2Ref	5,31 ± 0,750	530,61 ± 31,1	5,98 ± 0,251	50,8 ± 0,98	$3{,}89{\cdot}10^{-4}$	321
SBR EPDMd20	7,66 ± 0,974	514,49 ± 138	4,42 ± 0,128	53,5 ± 1,05	$8{,}18{\cdot}10^{-4}$	139
SBR EPDMd20 SiO_2	6,57 ± 1309	430,14 ± 19,4	6,55 ± 0,270	56,5 ± 1,87	$5{,}43{\cdot}10^{-4}$	237
SBR EPDMd40	7,87 ± 0,567	464,96 ± 28,6	6,88 ± 0,215	55,3 ± 1,03	$9{,}06{\cdot}10^{-4}$	123
SBR EPDMd40 SiO_2	9,29 ± 0,556	591,32 ± 45,6	12,82 ± 0,319	65,3 ± 1,21	$9{,}11{\cdot}10^{-4}$	157
SBR EPDMd50	6,56 ± 0,341	469,04 ± 17,8	6,58 ± 0,990	56,3 ± 1,04	$7{,}64{\cdot}10^{-4}$	132
SBR EPDMd50 SiO_2	4,61 ± 0,190	183,68 ± 9,70	10,72 ± 1089	69,5 ± 1,22	$1{,}35{\cdot}10^{-3}$	190
SBR EPDMd60	5,23 ± 1640	340,62 ± 59,1	2,51 ± 0,508	58,8 ± 0,75	$1{,}15{\cdot}10^{-3}$	148
SBR EPDMd60 SiO_2	3,46 ± 0,279	188,19 ± 38,9	10,33 ± 1,47	72,3 ± 1,63	$1{,}25{\cdot}10^{-3}$	175

also observed when EPDM and SiO_2 are present together. The hardness in the SBR EPDMd20 sample increases by 13.5 % compared to the SBR reference sample. A similar increase is observed in the same samples with SiO2 (13.3 %). As the samples have a higher EPDMd content, the hardness also increases in both samples (SiO_2 and SiO_2-free). This increase persevere until the content of EPDMd reaches 60phr (42,3 % and 21,2 % respectively).

3.2. Structural analysis by FTIR

Figs. 5 and 6 show the spectral regions within 1800 and 1300 cm^{-1} and 1200 and 600 cm^{-1} respectively, corresponding to the following samples: SBR ref, SBR SiO_2 ref, SBR EPDMd60 and SBR EPDMd60 SiO_2.

Distinctive bands corresponding to the various components present in these samples can be discerned. The doublet 1736–1729 cm^{-1} corresponding to unreacted stearic acid present in the samples, that stay in the surface. As commented previously the degree of crosslinking in the EPDMd samples is higher that SBR samples and this define this difference of intensities in the SBR ref and SBR SiO_2 ref. samples. The band at 1537 cm^{-1} and 1392 cm^{-1} (Delor et al., 1996; Virgili et al., 2005; Colom et al., 2009, 2018) are associated with Zn stearate ($ZnSt_2$) generated in the re-vulcanization process as a product of reaction of ZnO and stearic acid (StA). Both bands are higher in EPDMd samples due at the same reason explained previously, the CLK degree avoid the movement of $ZnSt_2$ and it remains in the surface. The 1474–1472 cm^{-1} band is associated to the methylene (-CH_2-) present in both SBR and EPDMd composites, where the -CH_2- of samples SBR-EPDMd is slightly displaced due to the interaction between the two components. While the band at 1462 cm^{-1} is more related to the free -CH_2- of butadiene (SBR), being more intense in the samples without SiO_2. The band at 1452 cm^{-1} is associate with CH_2 of norbornene (EPDM).

Fig. 6 shows the range most closely related to the bands of the SiO_2 group. In this spectral region, the assignment of bands is as follows: 1177 cm^{-1} to the EPDM group, 1062 cm^{-1} to the SiO_2, 962 cm^{-1} to the 1,4 trans-polybutadiene (SBR), 696 cm^{-1} to the mono substituted benzene rings (SBR) and 729 cm^{-1} to the -CH_2- of the polybutadiene (SBR) (Socrates, 2004).

Fig. 7 provides a comparative analysis of absorbance concerning the specified bands, governed by content (phr) of EPDMd and the presence of SiO_2. All these bands have been referenced in Fig. 5, observing in this comparative analysis of all the samples with SiO_2 that the EPDM content is significant in terms of the degree of crosslinking (band at 1177 cm^{-1}, assigned to EPDM). The higher the EPDM content, the higher the CLK degree, observing that the samples with higher EPDM content show higher absorbance in the bands assigned to $ZnSt_2$. Notably, our attention is drawn to a band, previously unexplored, manifesting at 1270–1260 cm^{-1} linked to C—O–C (StA and $ZnSt_2$).

This significant change, especially pronounced in the SBR EPDMd60 SiO2 sample, is related to the aforementioned affinity between EPDMd and SiO2 (Cañavate et al., 2010). This interaction, caused by the presence of BPO, is responsible for the different properties and behavior of samples containing SiO_2 compared to those without SiO_2. An evolution of the content of StA and ZnSt2 is observed due to crosslinking and to the amount of SiO_2 dispersed in the SBR matrix.

As the SiO_2 particles disappear from the SBR matrix because they are incorporated into the surface of the EPDM agglomerates, the number of particles decreases from the surface due to the lower degree of dispersion and the intensity of the band at 1262 cm^{-1} assigned to SiO_2 decreases (red box attached).

3.3. Thermal properties

As shown in Fig. 8a, corresponding to the SBR EPDMd samples without SiO_2, the presence of EPDMd increases the thermal decomposition temperature (TdT) and increases the ash content of the sample (up to 10 % in the SBR EPDMd60 sample). Fig. 8b shows the DTGA as a function of the temperature of the various elastomeric components of each sample. In the SBR ref the TdT is 450 °C and in the SBR EPDMd60 a peak at 475 °C appears, which corresponds to the TdT of the EPDMd (Mokhothu et al., 2014). However, it can be observed that, for low EPDMd contents (up to 40 phr) only a single TdT peak appears, which means that there is a good dispersion of EPDMd in the SBR matrix forming a homogeneous mixture. When EPDMd content is higher and reaches 50, 60 phr, two peaks are visible. These results imply that in these samples there are two phases, because the high EPDMd content form agglomerates (Colom et al., 2023) with a continuous arrangement which is the cause of the decrease of the mechanical properties. These data validate the microstructural arrangement, already exposed in the points above, that underlies the distinct mechanical properties exhibited by the samples according to their EPDMd content.

Comparing the thermograms of the samples containing SiO_2 (Fig. 8c), it is observed that the inorganic residue increases by 20 %, the TdT of the samples with SiO_2 decreases as a function of the EPDMd content when it is lower than 40phr (where a homogeneous phase is observed) and the TdT increases with EPDMd contents of 50 and 60 phr. As has been commented previously, this behavior is due to the formation of two phases, where the EPDMd phase, with a higher affinity for SiO_2, presents a TdT of 470 °C (lower than that of EPDMd witout SIO_2) and the SBR phase a TdT of 390 °C (Fig. 8d), very closed to SBR phase without SiO_2.

This difference in thermal behavior of SBR matrix and EPDMd agglomerates with SiO_2 corroborates the mechanical properties results obtained previously.

3.4. Morphological analysis by SEM

Figs. 9a and b corresponding to the samples of SBR ref and SBR SiO_2 ref show a homogeneous surface with some irregularities characteristic

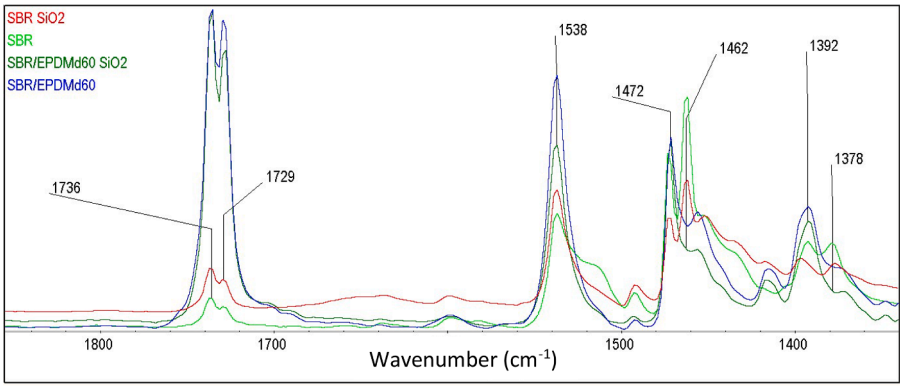

Fig. 5. Spectral region between 1800 and 1300 cm^{-1} of the SBR ref, SBR SiO_2 ref, SBR EPDMd60 and SBR EPDMd60 SiO_2 samples.

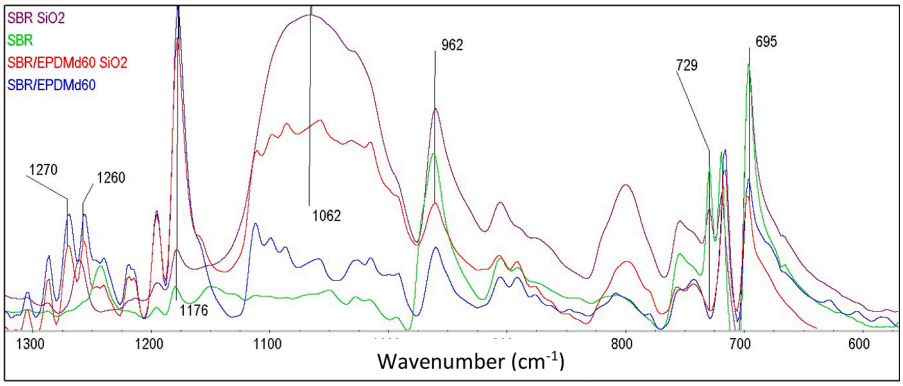

Fig. 6. Spectral region between 1200 and 600 cm^{-1} of the SBR ref, SBR SiO2 ref, SBR EPDMd60 and SBR EPDMd60 SiO_2 samples.

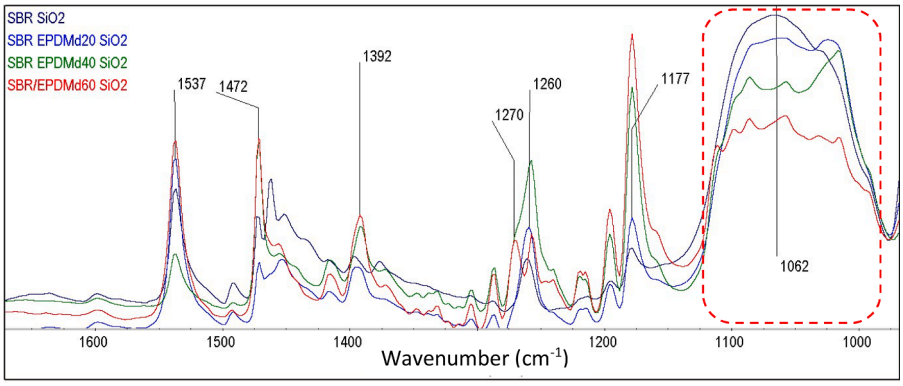

Fig. 7. Spectral region between 1600 and 1000 cm^{-1} of the samples SBR SiO_2 ref SBR EPDMd20 SiO_2, SBR EPDMd40 SiO_2 and SBR EPDMd60 SiO_2.

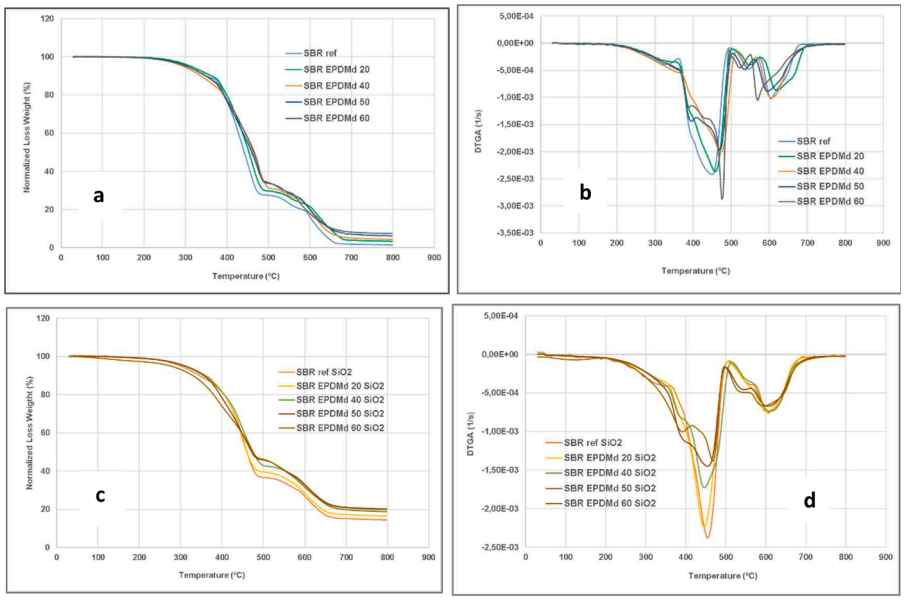

Figs. 8. a) TGA of samples without SiO_2; b) DTGA of samples without SiO_2; c) TGA of samples with SiO_2 and d) DTGA of samples with SiO_2.

of the additives incorporated in the SBR material, where the crystals of zinc stearate (Fig. 9a) and the SiO_2 particles are homogeneously distributed in the SBR matrix (Fig. 9b). The EPDMd (20phr) particles are distributed unevenly within the SBR matrix (Fig. 9c). As previously commented, SiO_2 particles has more affinity for EPDMd and therefore they are mostly located on the surface of the EDPMd.

This can be observed in the sample SBR EPDMd20 SiO_2 (Fig. 9d) where there are some white spots that prove the previous statement and even aids in the visualization of the distribution of the EPDMd inside the SBR matrix (some of them are enclosed in the dashed lines). The microphotographs in Figs. 9e and f show a 60phr of EPDMd, which generates more irregularities on the surface of the samples. As depicted in micrograph 9f, the incorporation of SiO_2 causes the enlargement of EPDMd. While there may be a significant continuity, the agglomerates

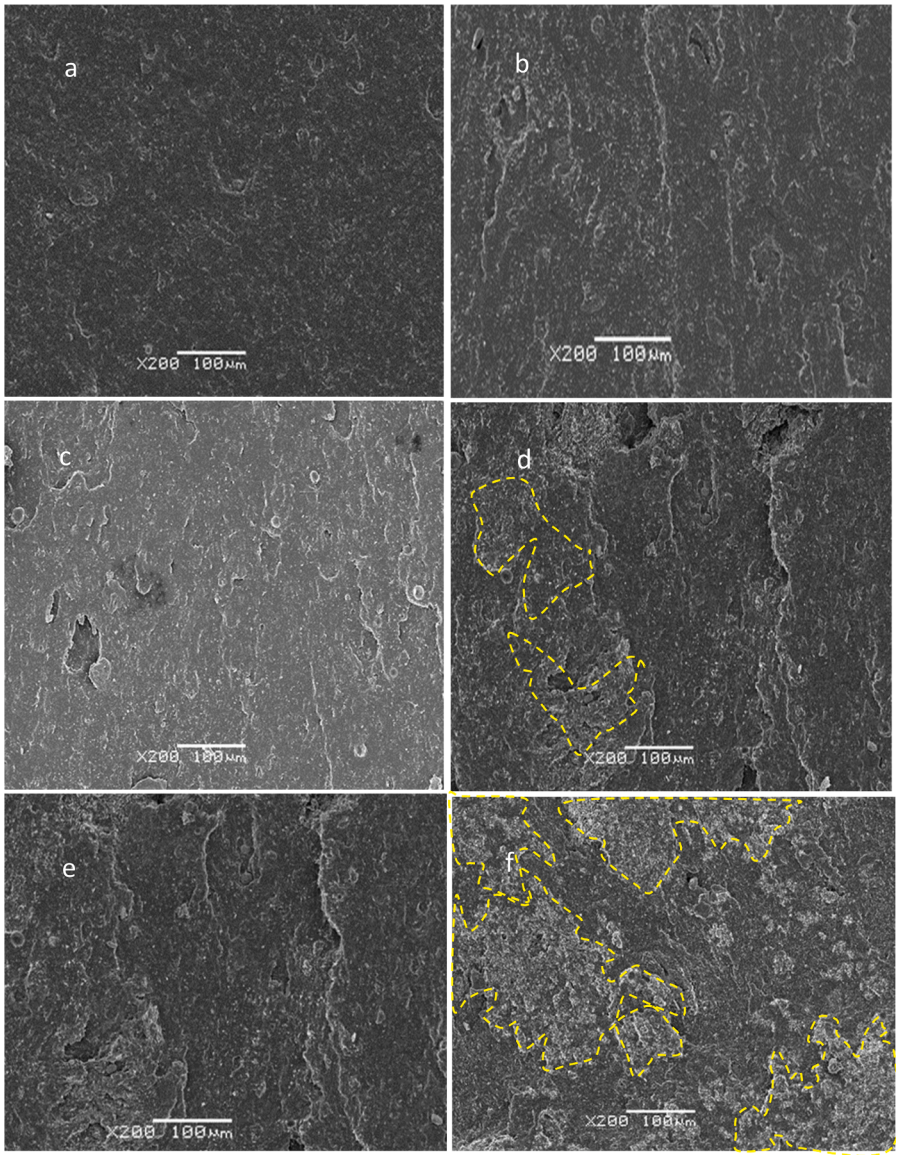

Fig. 9. SEM microphotographs of the elastomeric composites observed at x200 magnification: **a** SBR ref; **b** SBR SiO_2 ref; **c** SBR EPDMd20; **d** SBR EPDMd20 SiO_2; **e** SBR EPDMd60; **f** SBR EPDMd60 SiO_2 (yellow dash lines define the EPDMd-SiO_2 agglomerates).

give rise to relatively large entities, signaling that the mechanical properties of the samples with higher EPDMd content will start declining.

3.5. *Dielectrical Properties*

As shown in Table 3, the results of the dielectric measurements obtained at 70 °C and 130 °C confirm that the samples SBR ref, SBR SiO_2 ref, SBR EPDMd40 and SBR EPDMd40 SiO_2, are insulating at low frequencies and at temperatures of 70 °C and 130 °C (Marín-Genescà et al., 2023).

In this context, stable data for real permittivity (dielectric constant), imaginary permittivity and conductivity have been obtained. The conductivity values obtained for the SBR EPDMd40 composites, $1.23{\cdot}10^{-9}$ S/cm and $1.46{\cdot}10^{-9}$ S/cm, at 130 °C and 70 °C, respectively, are remarkable. These results are due to the MWS-type interfacial polarization at the SBR-EPDMd interface. The attenuation of the MWS effect caused by the addition of SiO_2 in the composites with high EPDMd content (SBR EPDMd40 SiO_2) is noteworthy. The addition of SiO_2 in these composites attenuates the SBR-EPDMd interfacial polarization effects, due to the presence of the SIO_2 layer around the EPDMd agglomerates formed in the samples, obtaining similar permittivity and conductivity values that the reference samples (SBRref and SBRref SiO_2). At high frequency increases the conductivity, due to the predominance of AC conductivity (Mujal-Rosas et al., 2012).

On the other hand, it is observed how the value of both permittivities (real and imaginary) decreases with increasing frequency. Finally, it should be noted that the permittivities reach moderate values for low frequencies, reaching 2390 (ε'') in SBR EPDMd40 composites. This value is so high due to the relevant MWS effect.

4. Conclusions

The results show that the devulcanization of EPDM and its incorporation into SBR enhance the mechanical properties of the blends when the content of EPDMd goes up to 40 phr. The devulcanization process facilitates successful interactions between the two components, resulting in significant microstructural changes that are reflected in the macroscopic properties of the composites

As in similar cases, the inclusion of SiO_2 reduces in general the tensile

Table 3
Real permittivity (ε'), Imaginary permittivity (ε'') and Conductivity are measured at 70 °C and 130 °C, in the range of frequencies, for SBR EPDMd composites: SBR ref, SBR SiO2 ref, SBR EPDMd40, SBR EPDMd40 SiO2.

Abbreviation samples	Freq. [Hz]	ε'	ε''	S (S/cm)	T (°C)
SBR ref	3,00E+06	3,81E-01	6,45E-02	1,04E-06	70
SBR SiO_2 ref	3,00E+06	3,11E-01	1,51E-02	1,15E-06	70
SBR EPDMd40	3,00E+06	4,33E+00	7,32E-01	5,70E-06	70
SBR EPDMd40 SiO_2	3,00E+06	4,50E-01	1,86E-02	9,19E-07	70
SBR ref	3,00E+06	3,69E-01	8,77E-02	1,06E-06	130
SBR SiO_2 ref	3,00E+06	3,19E-01	2,19E-02	1,14E-06	130
SBR EPDMd40	3,00E+06	4,93E-01	4,34E-02	8,49E-07	130
SBR EPDMd40 SiO_2	3,00E+06	3,72E+00	7,40E-01	4,70E-06	130
SBR ref	4,69E+02	2,62E+00	3,65E-01	4,34E-10	70
SBR SiO_2 ref	4,69E+02	2,03E+00	1,80E+00	5,40E-10	70
SBR EPDMd40	4,69E+02	6,59E+00	4,99E-01	1,46E-09	70
SBR EPDMd40 SiO_2	4,69E+02	2,16E+00	2,55E+00	7,31E-10	70
SBR ref	4,69E+02	2,40E+00	2,51E-01	3,71E-10	130
SBR SiO_2 ref	4,69E+02	3,43E+00	1,23E+00	7,09E-10	130
SBR EPDMd40	4,69E+02	5,45E+00	1,59E+00	1,23E-09	130
SBR EPDMd40 SiO_2	4,69E+02	5,56E+00	2,06E+00	1,30E-09	130
SBR ref	1,00E-02	1,74E+01	1,77E+02	9,86E-13	70
SBR SiO_2 ref	1,00E-02	4,08E+01	2,52E+02	1,42E-12	70
SBR EPDMd40	1,00E-02	1,89E+02	1,27E+03	7,15E-12	70
SBR EPDMd40 SiO_2	1,00E-02	1,59E+01	1,13E+01	1,04E-13	70
SBR ref	1,00E-02	1,49E+02	4,46E+03	2,48E-11	130
SBR SiO_2 ref	1,00E-02	3,68E+02	7,11E+03	3,96E-11	130
SBR EPDMd40	1,00E-02	6,38E+03	2,39E+04	1,38E-10	130
SBR EPDMd40 SiO_2	1,00E-02	5,84E+02	8,53E+03	4,75E-11	130

strength and elongation while increases the Young's modulus. However, this behavior deviates for compositions around 40phr EPDMd. This is related to the changes caused by the interaction of the SiO_2 with the EPDMd and the dispersion of this material within the SBR matrix. When EPDMd content exceeds 40 phr a pseudo-continuous phase forms, which weakens the composites decreasing the mechanical properties. These microstructural changes have been confirmed by FTIR, TGA and SEM analysis.

By the FTIR ATR technique, a displacement of the 1270–1261 cm^{-1} band associated to the SiO_2 group in the compounds is observed. This is a characteristic feature of the interaction between these components. Additionally, the FTIR analysis also shows that EPDMd increases the crosslinking degree hindering the exudation of StA and $ZnSt_2$. SEM microphotographs further confirm the affinity between EPDMd and SiO_2 due to devulcanization, showing a SiO_2 layer around the EPDMd agglomerates.

The dielectric measurements show remarkable values of the conductivity related to the MWS-type interfacial polarization at the SBR-EPDMd interface. In consonance with the previous results, there is an attenuation of the MWS effect caused by the addition of SiO_2 due to the presence of the SiO_2 layer around the EPDMd agglomerates formed in the samples, in the composites with high EPDMd content (SBR EPDMd40 SiO_2).

Analysing the different obtained properties, it can be concluded that SBR matrix composites with 20–40 phr of EPDMd, are suitable for automotive components such as dashboard, door handles and engine seals or gaskets.

Funding

The publication is part of grant PID2021-126165OB-I00 funded by MCIN/AEI/10.13039/501100011033 and by ERDF A way of making Europe by the European Union.

CRediT authorship contribution statement

X. Colom: Writing – review & editing, Writing – original draft, Visualization, Validation, Supervision, Resources, Project administration, Methodology, Investigation, Funding acquisition, Formal analysis, Data curation, Conceptualization. **M. Marín:** Writing – original draft, Resources, Investigation, Formal analysis. **M.R. Saeb:** Writing – original draft, Resources, Methodology, Investigation, Formal analysis. **K. Formela:** Writing – original draft, Visualization, Methodology, Investigation, Formal analysis. **J. Cañavate:** Writing – review & editing, Visualization, Validation, Resources, Methodology, Investigation, Funding acquisition, Formal analysis, Conceptualization.

Declaration of competing interest

I hereby declare that the disclosed information is correct and that no other situation of real, potential or apparent conflict of interest is known to me. I undertake to inform you of any change in these circumstances.

Data availability

Data will be made available on request.

References

Cañavate, J., Carrillo, F., Casas, P., Colom, X., Suñol, J.J., 2010. The use of waxes and wetting additives to improve compatibility between HDPE and ground tyre rubber. J. Compos. Mater. 44 (10), 1233–1245. https://doi.org/10.1177/0021998309351602.

Colom, X., Andreu-Mateu, F., Cañavate, F.J., Mujal, R., Carrillo, F., 2009. Study of the influence of IPPD on thermo-oxidation process of elastomeric hose. J. Appl. Polym. Sci. 114, 2011–2018.

Colom, X., Cañavate, J., Formela, K., Shadman, A., Saeb, M.R., 2021. Assessment of the devulcanization process of EPDM waste from roofing systems by combined thermomechanical/microwave procedures. Polym. Degrad. Stab. 183, 109450 https://doi.org/10.1016/j.polymdegradstab.2020.109450.

Colom, X., Carrillo-Navarrete, F., Saeb, M.R., Marin, M., Formela, K., Cañavate, J., 2023. Evaluation and rationale of the performance of several elastomeric composites incorporating devulcanized EPDM. Polym. Test. 121, 107976.

Colom, X., Marín-Genescà, M., Mujal, R., Formela, K., Cañavate, J., 2018. Structural and physico-mechanical properties of natural rubber/GTR composites devulcanized by microwaves: influence of GTR source and irradiation time. J. Compos. Mater., 002199831876155 https://doi.org/10.1177/0021998318761554.

Delor, F., Lacoste, J., Lemaire, J., Barrois-Odin, N., Cardine, C., 1996. Photo- and thermal ageing of polychloroprene: effect of carbon black and crosslinking. Polym. Degrad. Stab. 53, 361–369.

de Sousa, F.D.B., Zanchet, A., Marczynski, E.S., Pistor, V., Fiorio, R., Crespo, J.S., 2022. Devulcanized EPDM without paraffinic oil in the production of blends as a potential application of the residues from automobile industry. J. Mater. Cycles. Waste Manage 22, 273–284.

Dubey, K.A., Bhardwaj, Y.K., Chaudhari, C.V., Bhattacharya, S., Gupta, S.K., Sabharwal, S., 2006. Radiation effects on SBR–EPDM blends: a correlation with blend morphology. J. Polym. Sci., Part B: Polym. Phys. 44 (12), 1676–1689.

Ellis, B., Welding, G.N., 1964. Estimation from swelling of the structure contribution of chemical reaction to the vulcanization of natural rubber. Rubber Chem. Technol. 37, 571–575.

Flory, P.J., Rehner, J., 1943. Statistical mechanics of crosslinked polymer networks I. rubberlike elasticity. J. Chem. Phys. 11, 512–520.
Graf, H.-J., Blend of EPDM and SBR using an EPDM of different origin as a compatibilizer. Patent US-6800691B2, 5/10/2004.
Gschwind, L., Jordan, C.-S., Vennemann, N., Susoff, M.L., 2023. Mechanochemical devulcanization of EPDM rubber waste. Correlation of process parameters with sol–gel analyses and revulcanization properties. J. Appl. Polym. Sci. 140, e53768. https://doi.org/10.1002/app.53768, 2023.
Hejna, A., Wiśniewska, P., Kowalkowska-Zedler, D., Korol, J., Kosmela, P., Marć, M., Ezzati, P., Szostak, M., Saeb, M.R., 2023. Waste printer ink as modifier for natural rubber/carbon black composites: no haste, use waste. Sustain. Mater. Technol. 38.
Hrnjak-Murgić, Z., Jelenčić, J., Bravar, M., Marović, M., 1997. Influence of the network on the interaction parameter in system EPDM vulcanizate–solvent. J. Appl. Polym. Sci. 65, 991–999.
https://www.transparencymarketresearch.com/ethylene-propylene-diene-monomer-rubber.html 2023 (access 11/09/2023).
https://www.researchandmarkets.com/report/ethylene-propylene-diene-monomer#reld0-5313607 2023 (access 11/09/2023).
Kazemi, H., Mighri, F., Park, K.W., Fard, F.S., Rodrigue, D., 2019. Vulcanization kinetics and properties of natural rubber hybrid composites based on maple/silica/carbon black. Elastomery, 4, 227–240.
Kraus, G.J., 1963. Swelling of filler-reinforced vulcanizates. J. Appl. Polym. Sci. 7, 861–871.
Lee, S.Y., Kim, J.S., Lim, S.H., Kim, D.H., Park, N.-H., Jung, J.W., Choi, J., 2020. The investigation of the silica reinforced rubber polymers with the methoxy type silane coupling agents. Polymers (Basel) 12, 3058.
Marín-Genescà, M., García-Amorós, J., Mudarra, M., Massagués Vidal, L., Cañavate, J., Colom, X., 2023. Insights into the structural and dielectric behavior of composites produced from EPDM waste processed through to a devulcanization method and SBR. ACS. Omega.
Marzocca, A.J., 2007. Evaluation of the polymer–solvent interaction parameter χ for the system cured styrene butadiene rubber and toluene. Eur. Polym. J. 43 (6), 2682–2689. https://doi.org/10.1016/j.eurpolymj.2007.02.034.
Mokhothu, T.H., Luyt, A.S., Messori, M., 2014. Preparation and characterization of EPDM/silica composites prepared through non-hydrolytic sol-gel in the absence and presence of a coupling agent. Express Polym. Lett. 8 (11), 809–822.
Mujal-Rosas, R., Marin-Genesca, M., Orrit-Prat, J., Rahhali, A., Colom-Fajula, X., 2012. Dielectric, mechanical, and thermal characterization of high-density polyethylene composites with ground tire rubber. J. Thermoplast. Compos. Mater. 25 (5), 537–559.
Ravishankar, P.S., 2012. Treatise on EPDM. Rubber Chem. Technol. 85 (3), 327–349. https://doi.org/10.5254/rct.12.87993.
Rooj, S., Basak, G.C., Maji, P.K., Bhowmick, A.K., 2011. New route for devulcanization of natural rubber and the properties of devulcanized rubber. J. Polym. Environ. 19, 382–390. https://doi.org/10.1007/s10924-011-0293-5, 2011.
Socrates, G., 2004. Infrared and Raman Characteristic Group Frequencies: Tables and Charts. John Wiley & Sons Inc, New York.
Virgili, L., Giantomassi, F., Pugnaloni, A., Mattioli-Belmonte, M., Natali, D., Tarsi, R., Conti, C., Tosi, G., Margutta, M., Bonora, M., Biagini, G., 2005. FT-IR and biological evaluations of native and artificially aged rubber mixes. Polym. Degrad. Stab. 87, 143–151.
Welker, M.F., Jacob, S., Jourdain, E., Wouters, G., Devorest, Y., Joshi, M., 2012. A new EPDM with improved processing characteristics for automotive hose. In: Hose Manufacturers' Conference 2011 Technical Meeting of the Rubber & Plastic News Conference August 23-24, 2011. Cleveland, Ohio, 246, pp. 22–29.
Wiśniewska, P., Wójcik, N.A., Ryl, J., Bogdanowicz, R., Vahabi, H., Formela, K., Saeb, M. R., 2023. Rubber wastes recycling for developing advanced polymer composites: a warm handshake with sustainability. J. Clean. Prod. 427.
Yun, J., Isayev, A., Kim, S., Tapale, M., 2003. Comparative analysis of ultrasonically devulcanized unfilled SBR, NR, and EPDM rubbers. J. Appl. Polym. Sci. 88, 434–441. https://doi.org/10.1002/app.11741.
Zanchet, A., L, N., Giovanela, M., Brandalise, R.N., Crespo, J.S., 2012. Use of styrene butadiene rubber industrial waste devulcanized by microwave in rubber composites for automotive application. Mater. Des. 39, 437–443.
Zedler, Ł., Colom, X., Cañavate, J., Formela, K., 2021. GTR/NBR/Silica composites performance properties as a function of curing system: sulfur versus peroxides. Materials (Basel) 14, 5345. https://doi.org/10.3390/ma14185345.
Zoltán, P.D., Pölöskei, K., 2021. Thermomechanical devulcanisation of ethylene propylene diene monomer (EPDM) rubber and its subsequent reintegration into virgin rubber. Polymers (Basel) 13 (7), 1116. https://doi.org/10.3390/polym13071116.